Ultrasonic attenuation in a quasicrystal studied by picosecond acoustics as a function of temperature and frequency

J.-Y. Duquesne and B. Perrin
LMDH, Université Pierre et Marie Curie, CNRS (UMR 7603), Boîte 86, 4 Place Jussieu, 75252 PARIS Cedex 05, France
(Received 4 March 2003; published 7 October 2003)

We report on the acoustic attenuation in an AlPdMn icosahedral quasicrystal between 15 and 300 K, in the tens of GHz range. High frequency coherent longitudinal acoustic waves are excited and detected by an optical ''pump and probe'' technique, in an interferometric configuration. Our results reveal that, at high temperature ($T>100$ K), the acoustic attenuation is rather small, close to the attenuation in crystals and much smaller than in disordered solids. We stress that Akhieser processes (phonon-phonon interactions) must be active in quasicrystals and give the correct behavior and order of magnitude of the acoustic attenuation, at high temperature. At low temperature, departure from the standard behavior arising from phonon-phonon interaction is not understood.

DOI: 10.1103/PhysRevB.68.134205 PACS number(s): 61.44.Br, 62.65.+k, 63.20.Ry

I. INTRODUCTION

The lattice dynamics of quasicrystals is a challenging problem in solid state physics. The structure of quasicrystals exhibits a long range order which can be described using periodic structures in a higher dimensional space. Nevertheless, no powerful concept, equivalent to the Bloch theorem in crystals, can be used to describe the vibrational excitations in quasicrystals. However, much theoretical and experimental work has been devoted to this problem (for a review, see Ref. 1). The general agreement is that the character of the lattice excitations is, strictly speaking, critical in three-dimensional icosahedral solids. Critical modes decay on the average like a power law around a main site but can peak locally at several distant surrounding sites.[2] They are neither extended (as in periodic solids) nor localized (with an exponential decay around some site, as in disordered solids). However, at low frequency, the modes cannot practically be distinguished from really extended modes and are similar to the acoustic modes of crystals. Inelastic neutron[3] and x-ray scattering[4] experiments set the limit between high and low frequencies around a few THz. The acoustic attenuation and the thermal properties (dilation, heat capacity, thermal conductivity) are intimately related to the lattice excitations. In dielectric crystals, they can be explained, at least qualitatively, in a common framework dealing with extended lattice excitations (Bloch state phonons). In disordered dielectric solids (glasses), additional processes (tunneling states, thermal activated relaxations, soft modes, etc.) must be introduced to explain the thermal properties or the acoustic attenuation. In quasicrystals, the thermal conductivity, internal friction and sound velocity versus temperature are found to be glasslike at low temperature and have been explained within the phenomenological model of two level tunneling states.[5] At higher temperature, thermal data are available[6,7] but, to our knowledge, no ultrasonic absorption experiment has been reported yet. Mechanical spectroscopy data from 100 to 1000 K (1 Hz to 3 kHz) are also available and reveal thermal activated processes.[8] In the present paper, we report on acoustic experiments performed in a single *i*-AlPdMn quasicrystal, between 15 and 300 K, in the tens of GHz range.

II. EXPERIMENTAL PROCEDURE

The sample is a plate cut from a single icosahedral quasicrystalline domain $Al_{68.2}Pd_{22.8}Mn_{9.0}$ grown using the Czochralsky technique.[9] The faces are normal to a twofold axis and are polished flat and parallel. The thickness of the sample is 118 μm at room temperature. The wedge angle can be estimated using a mapping of the round-trip acoustic time versus the acoustic path location and is found to be about 4×10^{-4} rd. The surface roughness was estimated using an atomic force microscope. Small areas (7.5×7.5 μm^2) were investigated and the rms roughness was found to be around 4 nm. In order to compare the attenuation data, we also studied two Si[100] crystalline samples with low impurity content (phosphorus dopant). The samples are 110 and 198 μm thick with resistivity ρ: $165<\rho<240$ and $500<\rho$ Ω cm, respectively. The experiments are performed in a continuous-flow cryostat.

The experimental method we chose to perform sound absorption measurements is the so-called picosecond ultrasonics technique[10] which combines the use of short laser pulses and an optical pump-probe technique. A Ti:sapphire modelocked laser delivers linearly polarized pulses with a duration of 200 fs. A first laser pulse (the pump) is focused to a diameter of 18 μm on a thin (30 nm) aluminum film deposited on the sample. The film absorbs a fraction of the energy and generates a longitudinal acoustic pulse. This pulse propagates in the sample and gives rise to a series of echoes which are detected by a second, time delayed, laser pulse (the probe). The probe is focused to a diameter of 24 μm. The pump and probe wavelength is 750 nm. This technique has been mainly used in very thin films where the typical round-trip time is in between a few tens up to a few hundreds picoseconds. However it has been shown[11] that much thicker films corresponding to round-trip times above 100 ns can also be studied with such a technique if the repetition rate of

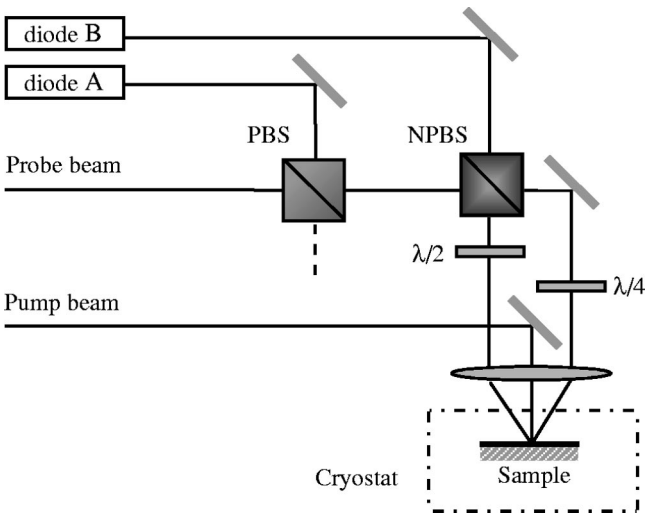

FIG. 1. ''Pump and probe'' picosecond acoustics setup, in a Sagnac interferometric configuration. (λ/2, half-wave plate; λ/4, quarter-wave plate; PBS, polarizing beamsplitter; NPBS, nonpolarizing beamsplitter.)

the laser has a good stability. The time delay T between two successive pulses of our laser source is typically around 12.2 ns, which means that for a delay t between the probe and the pump we can detect any event occuring at times $t+nT$ (n is an integer). The thickness of our AlPdMn sample was adjusted to get travel times for the first and second echoes of 35 and 70 ns, respectively. In such a way the echoes are detected with $n=3$ or 6 and appear, on the records, in an area where the thermal background is quite flat just before the time where pump and probe coincide. Acoustic echoes induce changes in the refractive index of the aluminum film (photoelastic effect) but also displacement of the surface; the photoelastic effect contributes to both real and imaginary parts of the relative changes or the reflection coefficient r which can be written as $(\Delta r/r)(t)=\rho_e(t)+i\phi(t)$ while the surface motion contributes only to the imaginary part ϕ. Interferometric detection[12,13] can independently measure ρ_e and ϕ. At low frequency the displacement contribution to the reflectivity change becomes larger than the deformation contribution and consequently ϕ is expected to be larger than ρ_e. Since high frequencies (~100 GHz) are highly damped at room temperature we use an interferometric detection to measure the imaginary part. To overcome the fluctuations of the refractive index due to the helium flow in the cryostat cell we also chose a Sagnac interferometer already described in Ref. 14 and in Fig 1.

After the polarizing beamsplitter, the probe beam is split by a nonpolarizing beamsplitter in two equal parts which propagate in the same loop along opposite directions. The sample is located within the loop in a nonsymmetrical position in such a way that the two beams reach the sample at different times t and $(t+\theta)$ compared to the pump beam; the delay θ between the two beams is 800 ps. Another asymmetry is introduced by the half- and quarter-wave plates: the half-wave plate rotates the beam polarization by 90 degrees in such a way that the counter propagating beams in the loop pass through the quarter-wave plate with a polarization either

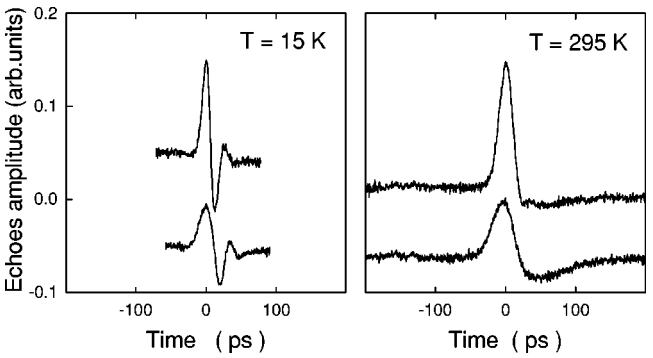

FIG. 2. First (upper) and second (lower) acoustic echoes at 15 and 295 K. For clarity, the echoes are arbitrarily translated along the time and amplitude axis.

parallel to the ordinary or to the extraordinary optical axis of the plate. After the loop the two beams interfere and are detected by two photodiodes A and B. Due to the $\pi/2$ phase shift introduced by the quarter-wave plate between the beams propagating in opposite directions it can be shown, assuming that the nonpolarizing beamsplitter is perfect, that the photodiode signals are

$$S_A(t)=\tilde{\rho}_e(t)\pm\tilde{\phi}(t), \tag{1}$$

$$S_B(t)=\tilde{\rho}_e(t)\mp\tilde{\phi}(t), \tag{2}$$

where $\tilde{\rho}_e(t)=\rho_e(t+\theta)+\rho_e(t)$ and $\tilde{\phi}(t)=\phi(t+\theta)-\phi(t)$. The imaginary part is measured from $S_A-S_B=\pm 2\tilde{\phi}$. The sign depends on the orientation of the quarter-wave plate. The pump is modulated at 1 MHz (duty factor 20%) and the induced change $\Delta r/r$ is detected with a lock-in amplifier; the sensitivity in surface displacement detection is estimated to be 5×10^{-6} nm.

Due to the very low thermal conductivity of AlPdMn (0.1 to 1.5 $\mathrm{W\,m^{-1}\,K^{-1}}$ from 10 to 300 K) (Refs. 5 and 7) and the small volume of the sample, special care must be payed to dc and ac heating problems. On the one hand, the ac heating (at 1 MHz) contributes to $\Delta r/r$ much more than the acoustic echoes but fortunately the differential detection of $\tilde{\phi}(t)$ gives a natural way to subtract this thermal background. On the other hand, low energy laser pulses must be used to reduce the dc heating. The dc heating is evaluated using the acoustic

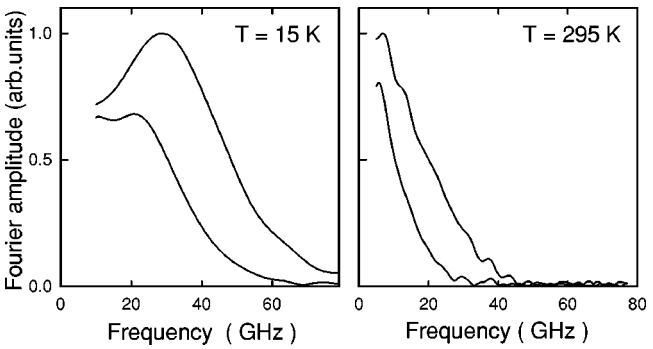

FIG. 3. Fourier transforms of the first (upper) and second (lower) echoes at 15 and 295 K.

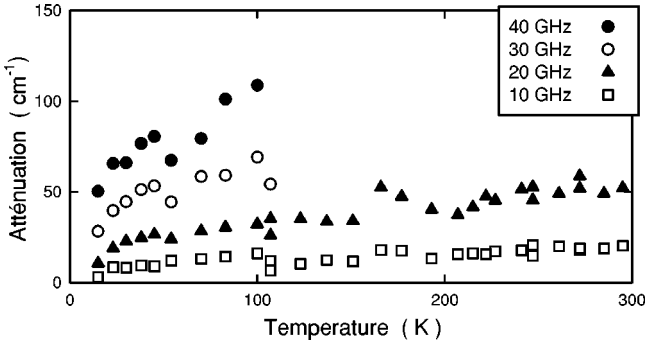

FIG. 4. Attenuation of longitudinal waves vs temperature in i-$Al_{68.2}Pd_{22.8}Mn_{9.0}$ at various frequencies.

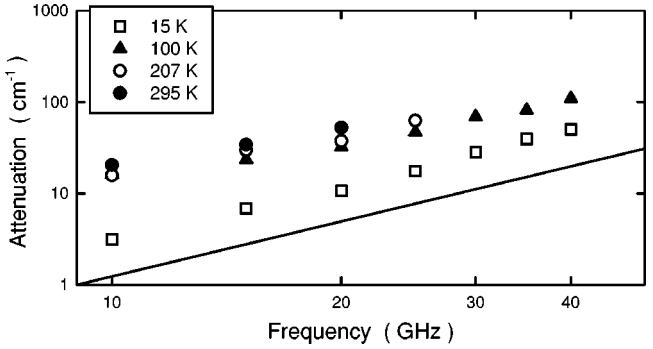

FIG. 5. Attenuation of longitudinal waves vs frequency in i-$Al_{68.2}Pd_{22.8}Mn_{9.0}$ at various temperatures. The full line displays a quadratic variation.

velocity variation versus incident mean energy. Above 100 K, the pump energy incident on the sample is $E_p = 0.7$ nJ per pulse, and each probe pulse energy is $E_s = 0.04$ nJ. At 295 K, the steady-state heating is found to be about 10 K. Below 100 K, we reduce the incident energies down to the point where no acoustic velocity change is observed at 15K: $E_p = 0.3$ and $E_s = 0.03$ nJ, per pulse. The temperature of the sample is then estimated to be only a few degrees above the thermometer temperature.

III. RESULTS

Figure 2 displays the first and second echoes that we observe at 15 and 300 K. We checked that no nonlinear effect is induced. For that purpose, we varied the energy of the pump pulses while adjusting the modulation duty factor in order to keep a constant mean incident energy and, then, a constant steady-state heating. No echo deformation is observed and the magnitude of the echoes is proportional to the energy of the pump pulses. We expected the echoes to superpose on a flat baseline because the round-trip acoustic time is such that they are probed more than 9 ns after the last pump pulse. Under such conditions, the shift that we observe between the baselines before and after the acoustic echoes does not come from the thermal background but from the echo shape. This shift is attributed to the details of the echoes building up and is not further analyzed. In order to perform a quantitative analysis, we compute the Fourier transform after subtraction of a linear background from the raw data. Clearly, the frequency content of the echoes is higher at low temperature. Figure 3 displays the Fourier amplitudes. The acoustic attenuation is then computed from the ratio of the Fourier amplitude of the first and second echoes.[15] Figure 4 displays the attenuation versus temperature, at various frequencies, between 15 and 295 K. The attenuation decreases linearly with temperature between 300 and 30 K. It seems that below 30 K (at 20 GHz) the attenuation decrease is becoming steeper. Unfortunately we could not perform experiments below 15 K in order to test this point. Figure 5 displays the attenuation versus frequency, at various temperatures, between 10 and 40 GHz. The variation of attenuation is roughly quadratic.

IV. DISCUSSION

Two sources of acoustic attenuation α must be considered: intrinsic microscopic processes giving a true acoustic attenuation and extrinsic sources originating from macroscopic defects, giving an apparent attenuation (poor parallelism, surface roughness, etc.). The nonparallelism effect was computed and found to be negligible.[21] In principle, the surface roughness contribution can be estimated by making measurements on a series of samples with identical surface condition and different thickness. We did not performed such experiments but we notice that the rms surface roughness (4 nm) is much smaller than the shortest investigated acoustic wavelength (160 nm at 40 GHz). Altogether, the effect of the different extrinsic sources can be assumed as temperature independent and their contributions can be estimated, at every frequency, as a residual attenuation at 0 K. Unfortunately, our experiments do not extend to sufficiently low temperature to make it possible to measure this residual attenuation. Nevertheless, we observe that the attenuation at 15 K is smaller than the attenuation at high temperature. At 20 GHz and above 100 K, $[\alpha(T) - \alpha(15\ \mathrm{K})]$ is more than 70% of the total attenuation $\alpha(T)$. Therefore, above 100 K, the main contribution to the attenuation comes from intrinsic processes. It is interesting to compare the attenuation in i-AlPdMn with the attenuation in other solids. Table I gives various data at room temperature. We have quoted an amorphous metallic film (a-TiNi), covalent glasses (a-SiO_2, a-As_2Se_3) and crystalline dielectric solids (c-SiO_2, c-Si). At 300 K, the attenuation in i-AlPdMn is much smaller than in the amorphous metal or in the covalent glasses. On the contrary, it is quite close to the attenuation we measured in crystalline Si. It is also close to the attenuation in crystalline SiO_2. (To our knowledge, no data are available in c-SiO_2 at 20 GHz and 300 K. However, using existing data and assuming a quadratic variation of the attenuation versus frequency, one predicts 60–120 cm^{-1} at 20 GHz and 300 K in c-SiO_2.) Moreover, we have previously noted that extrinsic processes could give a small contribution to the total attenuation. Then the actual intrinsic attenuation in i-AlPdMn could still be slightly smaller than measured. Therefore, from the point of view of the acoustic attenuation, i-AlPdMn compares to dielectric crystalline solids, not to disordered solids, at room temperature.

In crystalline solids, the interaction of acoustic waves with the thermal phonons is an efficient process for sound absorption.[21–23] It can be described at high temperature using

TABLE I. Longitudinal wave attenuation in different solids, at 300 K. PU, BS, and BPU stand for picosecond ultrasonics, Brillouin scattering, and Brillouin scattering using picosecond ultrasonics, respectively.

	a-TiNi	*a*-SiO_2 (film)		*a*-SiO_2 (bulk)		*a*-As_2Se_3	*c*-SiO_2		Si [100]	*i*-AlPdMn
α (cm^{-1})	600	3200	5600	1500	1000	6900	230	380	80	50
F (GHz)	30	30	40	35	30	30	40	35	20	20
Method	PU	PU	PU	BS	BPU	PU	BS	BS	PU	PU
Ref.	16	15	15	17	18	10	19	20	This work	This work

a Boltzmann equation approach.[23] Within the collision time approximation the attenuation α of an acoustic wave writes, if $\omega\tau \ll 1$,

$$\alpha = \frac{CT\omega^2\tau}{2\rho s^3}\left[(\langle\gamma^2\rangle - \langle\gamma\rangle^2) + \left(\langle\gamma\rangle^2 \frac{\langle v^2\rangle}{s^2} \right) \right], \qquad (3)$$

where C is the specific heat per unit volume of the crystal, T the temperature, ρ the mass density, τ the mean lifetime of the thermal excitations. $\omega/2\pi$ and s are the frequency and velocity of the sound wave. Here, the $\langle\ \rangle$ brackets stand for thermal averages. For example, we have

$$\langle\gamma\rangle = \sum_\lambda \frac{C_\lambda}{C}\gamma_\lambda, \qquad (4)$$

and similar expressions for $\langle\gamma^2\rangle$ and $\langle v^2\rangle$ where λ indexes all the vibrational modes. C_λ, γ_λ and v_λ are respectively the specific heat, the Grüneisen parameter (relative to the longitudinal deformation induced by the wave) and the group velocity of the λ mode.

Equation (3) displays two contributions to sound absorption, corresponding to the two sets of ( ) brackets. The first one corresponds to the Akhieser process and the second one to the thermoelastic effect. In the Akhieser mechanism, the acoustic wave acts as an external field which modulates the energies of the thermal lattice excitations through the Grüneisen parameters. These excitations readjust their energy distribution via anharmonic interactions on the time scale of the collision time τ and this delay gives rise to sound absorption. In the derivation of the Akhieser contribution, the character of the thermal lattice excitations does not play any part. Thus we stress that the Akhieser mechanism must be active, at room temperature, whatever the true nature of the lattice thermal excitations is (extended, localized, critical, etc.). In particular, it must be active in quasicrystals and the first part of Eq. (3) gives correctly the contribution α_A of the Akhieser mechanism,

$$\alpha_A = \frac{CT\omega^2\Gamma^2\tau}{2\rho s^3}, \qquad (5)$$

where $\Gamma^2 = \langle\gamma^2\rangle - \langle\gamma\rangle^2$. The thermoelastic absorption arises from heat flow between the regions of compression and rarefaction induced by the acoustic wave. In crystals, the heat is carried by extended and propagating lattice excitations. This shows up in Eq. (3) through the average group velocity v of the phonons. In quasicrystals, the nature of the lattice excitations is different so that the second part of Eq. (3) is no longer valid as it stands and should be modified. But this term can still be estimated by the macroscopic expression

$$\alpha_{th} = \left(\frac{C_{11}+2C_{12}}{C_{11}} \right)^2 \frac{\chi\rho T\beta^2\omega^2}{2sC^2}, \qquad (6)$$

where C_{11} and C_{12} are the elastic modulus, χ is the thermal conductivity, and β the linear dilation coefficient.

Using Eq. (6) and existing data,[5,7,24] we find that the thermoelastic contribution is negligible ($\alpha_{th} < 1\ cm^{-1}$, at 20 GHz, over the whole temperature range). Thus, we now only consider the Akhieser contribution α_A. We notice that the experimental results are in accordance with the quadratic frequency variation displayed by Eq. (5). At room temperature, the specific heat is close to the Dulong-Petit expectation for the specific heat due to lattice excitations:[6] $C = 2.7 \times 10^6\ J\,m^{-3}\,K^{-1}$. Using $\rho = 5130\ kg\,m^{-3}$, $s = 6500\ m\,s^{-1}$, and $\alpha = 50\ cm^{-1}$ at 20 GHz and 300 K, we find $\Gamma^2\tau = 1.1 \times 10^{-12}$ s at 300 K. This value compares to typical values in crystals where Γ and τ are of the order of 10^0 and 10^{-13} s, respectively (in *c*-Si, using $\alpha = 80\ cm^{-1}$ at 20 GHz and published data, we find $\Gamma^2\tau = 2.4 \times 10^{-12}$ s at 300 K). Moreover, the Grüneisen constant $\langle\gamma\rangle = 1.7$ which can been extracted from dilation[24] is also close to typical values in crystals. We can check that our result is consistent with the assumption $\omega\tau \ll 1$. When the temperature is lowered, the same calculation can be performed consistently down to $T \sim 100$ K. Figure 6 displays a logarithmic plot of $\Gamma^2\omega\tau$ between 100 and 300 K, derived using the attenuation at 20 GHz and the ex-

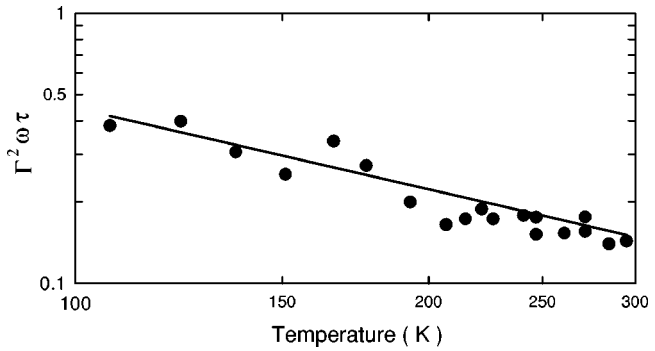

FIG. 6. $\Gamma^2\omega\tau$ derived from Eq. (5), using the attenuation measurement at 20 GHz (see the text). The full line is a T^{-1} function.

perimental specific heat.[6] In that range, we notice that $\Gamma^2\omega\tau$ varies roughly as T^{-1}. Thus, assuming that Γ is constant between 100 and 300 K, τ is found to vary as T^{-1} at high temperature. That kind of behavior is well known in crystals and arises from the density of phonons being proportional to the temperature, at high temperature.[25] In quasicrystals, the density of lattice excitations must also be proportional to the temperature, at high temperature, so that the T^{-1} variation of τ is also expected. Then, at high temperature ($T>100$ K), we suggest that anharmonic processes exhibit similar features in crystals and quasicrystals. The Akhieser mechanism alone can explain the observed acoustic attenuation in our frequency range. The Grüneisen constants and the thermal excitations lifetime τ have the usual order of magnitude. Moreover, τ behaves as T^{-1}. In contrast with the acoustic attenuation, the thermal conductivities in quasicrystals and crystals have very different behaviors. In quasicrystals, the thermal conductivity is mainly dominated by the localization length of the vibrational modes and cannot be used to derive the thermal excitations mean lifetime.

Equation (3) is only valid if $\omega\tau \ll 1$. When the temperature is lowered, the Boltzmann equation approach remains valid but the absorption can no longer be clearly divided in Akhieser and thermoelastic contributions. In crystals, if $\omega\tau \gg 1$ the Landau-Rumer regime is reached. In this regime, the acoustic wave is regarded as a collection of phonons decaying because of their anharmonic interaction with the thermal phonons. The transition between the Akhieser and Landau-Rumer regimes has been described by various models which rely on a detailed analysis of the phonon-phonon interactions. In this case, the true nature of the lattice excitations is important for a rigorous calculation of the absorption. For this reason, the interpolation formulas cannot be used in quasicrystals; a detailed theory would require a precise knowledge of the thermal modes, as well as of their coupling and mean lifetimes. However, we still expect the attenuation to drop below some temperature because of the depletion of the thermal lattice modes. From our measurements, it seems that there is an attenuation drop around 30 K, but additional experiments extending to much lower temperature should be performed to confirm this point.

While the attenuation at room temperature has the same order of magnitude as in dielectric crystalline solids, we should notice[26] that this is no longer true below 100 K. Moreover, the attenuation still varies as ω^2 down to 15 K so that, surprisingly, no crossover to a new regime is observed. Then, clearly, at low temperature, the attenuation does not behave as in crystalline dielectric solids.

The discrepancy may be searched for either in the particular features of the phonon-phonon interaction in quasicrystals or in other sound absorption sources. At low temperature, other possible sources are the electronic scattering and the tunneling states scattering. The extrinsic residual attenuation due to macroscopic defects (surface roughness, etc.) must also be considered. The acoustic attenuation by interaction with conduction electrons is proportional to nl_e where n and l_e are the conduction electrons density and mean free path, respectively.[21] This value can be derived from measurements of the electronic conductivity. Using typical values,[7] we find that nl_e is small and that the contribution of the electronic processes to the attenuation is negligible (of the order of 10^{-2} cm^{-1} at 20 GHz). Acoustic experiments[27–29] in quasicrystals at low temperature have revealed tunneling states (two-level systems) with a broad distribution of energy splitting, responsible for sound absorption. Above a few Kelvin, the acoustic attenuation is dominated by a relaxation process and can be computed using the phenomenological theory derived for glasses,[30] given the deformation potential B and the tunneling states density P. Using[28] $PB^2/\rho s^2 = 2.2\times 10^5$ and a density $P = 2\times 10^{45}$ J^{-1} m^{-3} which is typical of amorphous metals,[29] we find that the tunneling states contribution to the absorption is negligible in our temperature range. Finally, at low temperature, the extrinsic residual attenuation could blur possible phonon-phonon interactions. To settle this point, further experiments at lower temperature or on series of samples with different thicknesses are necessary in order to evaluate both contributions.

V. CONCLUSION

We have measured the acoustic attenuation in the icosahedral quasicrystal $Al_{68.2}Pd_{22.8}Mn_{9.0}$, between 15 and 300 K, and in the tens of GHz range. We find that, above 100 K, the attenuation behavior compares more to crystals than to amorphous solids. In disordered solids, the Akhieser process alone cannot explain the acoustic attenuation. Other relaxation processes are active (thermal activation of localized excitations, structural relaxation etc.). In a quasicrystal, we stress that, on the contrary, the attenuation behavior between 100 and 300 K is consistent with an Akhieser relaxation process involving the relaxation of lattice modes perturbed by the acoustic wave. In this temperature range, the mean lifetime of the thermal excitations varies in the same way as in crystals, i.e., according to a T^{-1} law , and with the same order of magnitude ($\Gamma^2\tau \sim 10^{-12}$ s). Below 100 K, the frequency dependence of the attenuation is still quadratic so that we do not observe a crossover to a low temperature regime similar to the Landau-Rumer regime which exists in crystals. The behavior of the attenuation is not clearly understood in this temperature range. It would be interesting to perform experiments down to much lower temperature ($T \sim 1$ K).

[1] M. Quilichini and T. Janssen, Rev. Mod. Phys. **69**, 277 (1997).

[2] C. Sire, in *Lectures on Quasicrystals*, edited by F. Hippert and D. Gratias (Les Editions de Physique, Les Ulis, France, 1994), p. 505.

[3] M. de Boissieu, M. Boudard, R. Bellissent, M. Quilichini, B. Hennion, R. Currat, A.I. Goldman, and C. Janot, J. Phys.: Condens. Matter **5**, 4945 (1993).

[4] M. Krisch, R.A. Brand, M. Chernikov, and H.R. Ott, Phys. Rev. B **65**, 134201 (2002).

[5] E.J. Thompson, P.D. Vu, and R.O. Pohl, Phys. Rev. B **62**, 11 437

(2000).
[6] C. Wälti, E. Felder, M.A. Chernikov, H.R. Ott, M. de Boissieu, and C. Janot, Phys. Rev. B **57**, 10 504 (1998).
[7] A.L. Pope, T.M. Tritt, M.A. Chernikov, and M. Feuerbacher, Appl. Phys. Lett. **75**, 1854 (1999).
[8] M. Feuerbacher, N. Weller, J. Diehl, and K. Urban, Philos. Mag. Lett. **74**, 81 (1996).
[9] M. Boudard, E. Bourgeat-Lami, M. de Boissieu, C. Janot, M. Durand-Charre, H. Klein, M. Audier, and B. Hennion, Philos. Mag. Lett. **71**, 11 (1995).
[10] C. Thomsen, H.T. Grahn, H.J. Maris, and J. Tauc, Phys. Rev. B **34**, 4129 (1986).
[11] H.-Y. Hao and H.J. Maris, Phys. Rev. Lett. **84**, 5556 (2000).
[12] B. Perrin, B. Bonello, J.-C. Jeannet, and E. Romatet, Prog. Nat. Sci. **6**, 444 (1996).
[13] B. Perrin, C. Rossignol, B. Bonello, and J.-C. Jeannet, Physica B **263-264**, 571 (1999).
[14] B. Perrin, in *Systèmes Femtosecondes*, edited by P. Laporte and F. Salin (Publications de l'Université de Saint-Etienne, Saint-Etienne, France, 2001), pp. 65–89.
[15] T.C. Zhu, H.J. Maris, and J. Tauc, Phys. Rev. B **44**, 4281 (1991).
[16] C.J. Morath and H.J. Maris, Phys. Rev. B **54**, 203 (1996).
[17] R. Vacher, J. Pelous, and E. Courtens, Phys. Rev. B **56**, R481 (1997).
[18] H.-N. Lin, R.J. Stoner, H.J. Maris, and J. Tauc, J. Appl. Phys. **69**, 3816 (1991).
[19] R. Vacher and J. Pelous, Phys. Rev. B **14**, 823 (1976).
[20] J.P. Bonnet, M. Boissier, and A. Ait Gherbi, J. Non-Cryst. Solids **167**, 199 (1994).
[21] R. Truell, C. Elbaum, and B.B. Chick, *Ultrasonic Methods in Solid State Physics* (Academic Press, New York and London, 1969).
[22] T.O. Woodruff and H. Ehrenreich, Phys. Rev. **123**, 1553 (1961).
[23] H.J. Maris, in *Physical Acoustics*, edited by W.P. Mason and R. N. Thurston (Academic Press, New York and London, 1971), Vol. VIII, p. 279.
[24] C.A. Swenson, I.R. Fisher, N.E. Anderson, Jr., P.C. Canfield, and A. Migliori, Phys. Rev. B **65**, 184206 (2002).
[25] J.M. Ziman, *Electrons and Phonons* (Clarendon Press, Oxford, 1960), Chap. 8.
[26] M. Pomerantz, Phys. Rev. **139**, A501 (1965).
[27] N.O. Birge, B. Golding, W.H. Haemmerle, H.S. Chen, and J.M. Parsey, Jr., Phys. Rev. B **36**, 7685 (1987).
[28] N. Vernier, G. Bellessa, B. Perrin, A. Zarembowitch, and M. de Boissieu, Europhys. Lett. **22**, 187 (1993).
[29] F. Bert, G. Bellessa, A. Quivy, and Y. Calvayrac, Phys. Rev. B **61**, 32 (2000).
[30] J. Jäckle, Z. Phys. **257**, 212 (1972).